*Jaume Anguera, Aurora Andújar, Jeevani Jayasinghe. **High-Directivity Microstrip Patch Antennas Based on TMood-0 Modes**: Antennas and Wireless Propagation Letters, IEEE 2020. Vol.19, Nº1, p. 39-43* https://doi.org/10.1109/LAWP.2019.2952260

High-Directivity Microstrip Patch Antennas Based on TModd-0 Modes

Jaume Anguera, Aurora Andújar, Jeevani Jayasinghe
Engineering Department, La Salle Ramon Llull University, Barcelona, Spain.
Fractus Antennas, Barcelona, Spain.
Department of Electronics, University of Wayamba, Kurunegala, Sri Lanka

Abstract
High-directivity microstrip antennas are attractive for the line-of-sight communications due to their thin profile. In order to achieve a high-directive radiation pattern, the geometry of a patch operating at a TModd-0 mode is modified to minimize the effect of out-of-phase currents. Two high-directivity microstrippatch antennas operating at modified TM30 and TM50 modes are presented. They exhibit broadside radiation patterns with directivities of 15 and 18 dBi, respectively. The advantage of the proposed technique compared to an antenna array is that no feeding network is required, and thus, the design is simpler and avoids the losses caused by the feeding network.Aprototype to validate the proposed technique is built, achieving ameasured directivity of 14.6 dBi. The microstrip patch antenna has a total size of 3(λ/2)×3(λ/2), and its measured bandwidth is four times that of an equivalent array of microstrip patches operating in its fundamental mode.

Index Terms: High directivity, High – order TM modes, Microstrip antennas, TM Modes.

I. Introduction

Microstrip patch antennas are widely used for many practical applications due to their planar profile, flexibility for broadening the bandwidth, multiband operation, and miniaturization [1]. Examples can be found in the Global Positioning System applications and arrays for micro and macro cell formobile communications. For applications requiring a certain directivity, arrays of microstrip patches are proposed where several architectures, such as corporate and series-fed, have been proposed [2]. Furthermore, many efforts have been made to obtain a high directivity and a broadside radiation pattern with a single microstrip patch antenna in order to avoid a feeding network [3]–[24]. This approach simplifies the structure of the antenna, reducing space and weight and the residual radiation of the feeding network.

Although the radiation patterns of a classical microstrip patch antenna, such as a square, circular, or triangle, are broadside at some TM modes, the secondary lobes are as high as the main lobe (example: TM30 of a square patch). In this sense, fractal shapes have been proposed [3]–[8] to obtain broadside radiation patternswith directivities up to 18.6 dBi. Somemore approaches rely on superstrates and partially reflective surfaces [9]–[18], and higher directivities of about 20 dBi could be obtained. However, such antenna configurations need a superstrate above the microstrip patch, making the structure more complex. Moreover, optimization methods based on the genetic algorithms, have been employed to achieve high directivity and broadside modes reaching directivities of about 12 dBi [19], [20]. In [21] and [22], the patches loaded with the slots and the short pins are proposed to enhance directivity. However, the increment compared to the directivity of a patch operating in its fundamental mode is about 1.7 dBi, resulting in a directivity of 10.8 dBi. In [23] and [24], the slots are loaded on microstrip patches operating at the higher

This is a post-print (final draft post-refeering)
Published in final edited form as

Jaume Anguera, Aurora Andújar, Jeevani Jayasinghe. ***High-Directivity Microstrip Patch Antennas Based on TMood-0 Modes****: Antennas and Wireless Propagation Letters, IEEE 2020. Vol.19, Nº1, p. 39-43* https://doi.org/10.1109/LAWP.2019.2952260

order modes to reduce sidelobe levels, and directivities up to 13.2 dBi are achieved.
In contrast, this letter proposes a technique that is based on perturbing the shape of a microstrip patch in order to minimize the conductive portions supporting opposite currents. At the same time, the technique does not need a superstrate above it and can provide a directivity of 18 dBi.

This letter is structured as follows. The basic theory on how to obtain a high-directivity performance is discussed in Section II. An electromagnetic analysis of a microstrip patch antenna presenting the technique to strategically modify its geometry is presented in Section III. To corroborate the electromagnetic analysis, a prototype antenna is built, and results are shown in Section IV. In Section V, several directivity enhancement techniques are discussed. Finally, conclusions are drawn in Section VI.

II. Basic Theory

To achieve a high-directivity radiation pattern, the antenna should be large in terms of the wavelength [25]. Therefore, it is needed to operate in a higher order mode compared to the fundamental mode TM10. If a broadside radiation pattern is also an objective, TMeven-0 modes need to be avoided since they have a null at the broadside direction due to the out-of-phase current portions on the patch surface that cancel radiation in the broadside direction. Hence, in order to avoid a null at the broadside direction, the contribution of the in-phase and out-of-phase currents should not be equal. Therefore, this research focuses on analyzing TModd-0 current distributions.

(a)

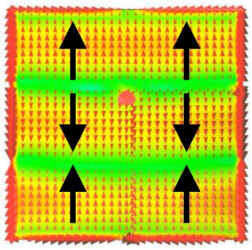

(b)

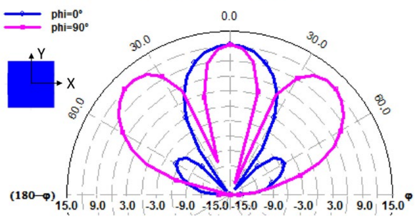

Fig. 1. Performance of the square-shaped antenna at a TM30 mode (*f* =2.41 GHz). (a) Current distribution. (b) Radiation pattern. Simulation considers an infinite ground plane. Patch size is 183 mm × 183 mm. It is placed on a 2 mm height air substrate. Black arrows are intentionally added to emphasize the current distribution.

Asquare-shaped patch placed on an air substrate with a height of 2 mm is simulated on a MoM-based code (IE3D). The patch is excited with a coaxial probe, and an infinite ground plane was considered in simulations. When the current distribution at a TM30 mode is computed using MoM, two in-phase current portions and one central out-of-phase current portion at the center of the patch can be observed [see Fig. 1(a)]. Since the out-of-phase current portion is weaker than the in-phase current portion (amplitude is similar, but the in-phase portion has twice the area), there is no null along the broadside direction, as happens at TMeven-0 modes. However, the problem of operating

This is a post-print (final draft post-refeering)
Published in final edited form as

Jaume Anguera, Aurora Andújar, Jeevani Jayasinghe. ***High-Directivity Microstrip Patch Antennas Based on TMood-0 Modes****: Antennas and Wireless Propagation Letters, IEEE 2020. Vol.19, Nº1, p. 39-43* https://doi.org/10.1109/LAWP.2019.2952260

at a TM30 mode is that the radiation pattern has two secondary lobes with the same amplitude as the main lobe, which reduce directivity [see Fig. 1(b)]. Hence, the goal is to reduce the secondary lobes to increase the directivity.

To demonstrate how those current portions determine the radiation pattern, the currents at the TM30 mode are modeled by an array of current portions. By using a basic array theory, the radiation pattern of the patch operating at the TM30 can be approximated by an array of three current portions similar to a current given at the fundamental mode TM10 as follows:

$$\vec{E} = \vec{E}_o \cdot \left(a_0 + a_1 \cdot e^{jk_y d} + a_2 \cdot e^{j2k_y d}\right) \qquad (1)$$

where *Eo* is the radiation pattern of a current portion at TM10 mode, *a*0 = *a*2 = 1 and *a*1 = –1; *a*0 and *a*2 represent the current portions with an in-phase current, and *a*1 the out-phase current portion; *ky* is the wavenumber in the *y*-direction as the array is aligned with the *y*-axis in this particular example (see Fig. 2); *d* is the distance between current portions, which is equal to *λ*g/2 (the three elements are in fact touching each other as the size of a patch (*L* × *L*) operating at TM30 is *L* = 3*λ*g/2), where *λ*g is the wavelength in the substrate of the microstrip patch.

The radiation pattern with this model considering *a*0 = *a*2 = 1, and *a*1 = –1 results in a radiation pattern with two secondary lobes as the TM30 mode. The results confirm the reliability of the model for analyzing radiation patterns with an array theory. Therefore, the model can be used to predict the radiation patterns of the other higher orders as well by adjusting the amplitudes *ai* in (1). For example, the radiation pattern at TM50 can be predicted by adjusting the amplitudes as follows: *a*1 = *a*3 = *a*5 = 1, and *a*2 = *a*4 = –1.
According to the array model, if the out-of-phase portion is 0 (*a*1 = 0), the radiation pattern changes drastically, where secondary lobes drop, and in consequence, directivity is increased by about 3 dB(see Fig. 2). Therefore, the objective is to minimize the out-of-phase current portion while maintaining the in-phase portions. In order to achieve this, removing the conductor in the area of the out-of-phase current portions is proposed as explained in Section III.

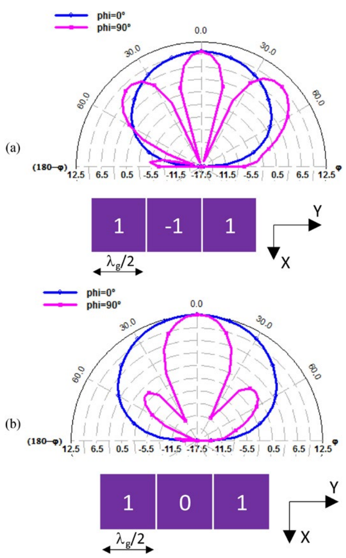

Fig. 2. Radiation patterns predicted using an array theory considering a patch operating in the fundamental modeTM10 and adjusting the amplitudes as shown on the boxes. (a) Directivity for the case *a*0 = *a*2 = 1, and *a*1 = –1 is *D* = 10 dBi. (b) Directivity for the case *a*0 = *a*2 = 1 and *a*1 = 0 is *D* = 12.8 dBi.

This is a post-print (final draft post-refeering)
Published in final edited form as

Jaume Anguera, Aurora Andújar, Jeevani Jayasinghe. ***High-Directivity Microstrip Patch Antennas Based on TMood-0 Modes****: Antennas and Wireless Propagation Letters, IEEE 2020. Vol.19, Nº1, p. 39-43* https://doi.org/10.1109/LAWP.2019.2952260

III. Perturbing TMood-0 Modes

In order to increase the directivity at TModd-0 modes, the out-of-phase current portions should be eliminated or at least minimized. In order to achieve this, the patch surface is removed in the out-of-phase portions while leaving some conductive strips connecting the in-phase portions. Two examples are shown: one at the TM30 mode, and the other at the TM50 mode (see Figs. 3 and 4). Both microstrip patches are placed on the same air substrate having a height of 2 mm, and they are fed with a coaxial probe.

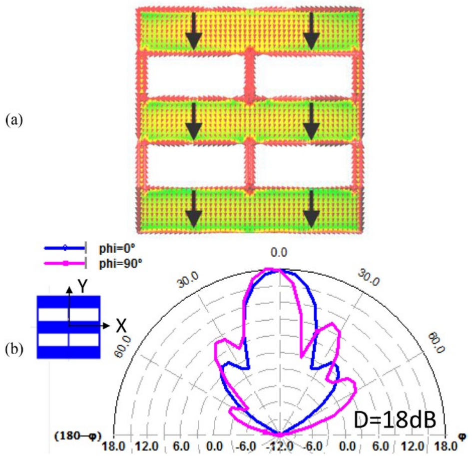

Fig. 3. Performance of the modified antenna at a TM30 mode. (a) Current distribution. (b) Radiation pattern. The patch is 183 mm × 183 mm on a 2 mm air substrate and is excited with a coaxial probe at (0, 20) mm, with (0, 0) being the center of the patch. *f* = 2.35 GHz. Black arrows are intentionally added to emphasize the current distribution.

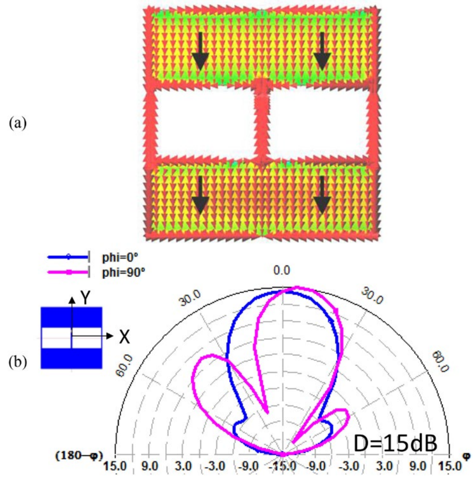

Fig. 4. Performance of the modified antenna at a TM50 mode. (a) Current distribution. (b) Radiation pattern. The patch size is 292 mm × 292 mm on a 2 mm air substrate and is excited with a coaxial probe at (0, 36) mm, with (0, 0) being the center of the patch. *f*=2.35 GHz. Black arrows are intentionally added to emphasize the current distribution.

For the operation at TM30, the in-phase portions are similar to that of the original patch. Since the out-of-phase current has been minimized, the term *a*1 in (1) is close to zero, and in consequence, the obtained radiation pattern at Φ = 90° is similar to that of the array model of Fig. 2. The directivity of this perturbed TM30 patch reaches 15 dB, whereas it was only 12.2 dB without the perturbation. This result is aligned with the increment of about 3 dB predicted by the array model, proving the usefulness of the array model.
An example at the TM50 mode is also presented (see Fig. 4). In this case, the number of openings on the patch surface is increased as the number of out-of-phase portion for a TM50 is two (see Fig. 4). A simulated directivity of 18 dB is demonstrated. The secondary lobes are due to the out-of-phase current flows along the thin strips (see Figs. 3 and 4).
It is interesting to note that the area of the patch operating at the TM50 mode is (5/3)2 compared to the area of the patch operating at the TM30 mode. This large area will result in an increment of 4.4 dB theoretically based on the directivity on an aperture [25], and in this case the increment is 3 dB.
From a practical perspective, it is worth pointing out that the opening on the patch is useful to include radio-frequency components, such as matching networks, filters, phase shifters, and amplifiers, as long as they do not perturb current distribution on the patch surface.

Jaume Anguera, Aurora Andújar, Jeevani Jayasinghe. ***High-Directivity Microstrip Patch Antennas Based on TMood-0 Modes****: Antennas and Wireless Propagation Letters, IEEE 2020. Vol.19, Nº1, p. 39-43* https://doi.org/10.1109/LAWP.2019.2952260

Besides directivity, radiation efficiency has also been computed for the two examples; radiation efficiencies are 95.0% and 95.5% for the TM30- and TM50-based antennas, respectively. Cross-polar discrimination (XPD) has been computed for the three cases (TM10, perturbed TM30, and perturbed TM50) at an angle, which has a gain 3 dB below the maximum, resulting in the XPD of 27.0, 18.7, and 21.8 dB, respectively.
Finally, the arrays of the square patches with uniform excitation operating in its fundamental mode TM10, occupying the same area of the perturbed TM30 (array of 2 × 2 elements occupying 183 mm × 183 mm) and TM50 (array of 3 × 3 elements occupying 292mm×292 mm) patches, are simulated.
The directivities are 15.5 and 19.1 dB, respectively, showing that a similar directivity can be obtained with no feeding network with the technique presented in this letter

IV. Application of a TM30 Perturbation

In order to validate the electromagnetic analysis, a highdirective patch at 2.6GHzis presented.To obtain a high-directive broadside pattern, a TM30 patch is designed. The patch is designed on a foam substrate having a relative permittivity *εr* = 1 and a 2 mm thickness. Thus, the size of the patch is determined as follows:

$$f_{mn} = \frac{c}{2\sqrt{\varepsilon_r}}\sqrt{\left(\frac{m}{L}\right)^2 + \left(\frac{n}{W}\right)^2}. \qquad (2)$$

A square patch (*L* = *W*) is considered on a foam substrate of *εr* = 1, *L*=3/2 ・*λ* at theTM30 mode where *λ* is thewavelength in the vacuum. Since the central frequency of operation is 2.6 GHz, *L* = 173 mm. The fringe fields have been neglected in this calculation.
Following the guidelines presented in Section III, the out-ofphase currents are removed by removing the conductive portion that supports the out-of-phase current, which corresponds to *L*/3 (see Fig. 5).
In Section III, itwas demonstrated that a patch operating under a perturbed TM30 mode is comparable to an array occupying the same area with the advantage that no feeding network is required. If the array has a uniform phase distribution, an impedance bandwidth of the array is the same as the bandwidth of the basic

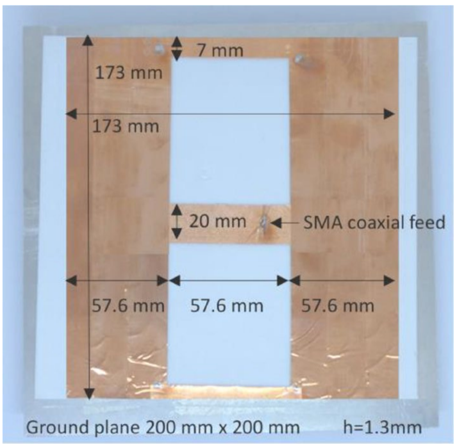

Fig. 5. Prototype of a patch operating at a perturbed TM30 mode. The patch is fed by a coaxial probe.

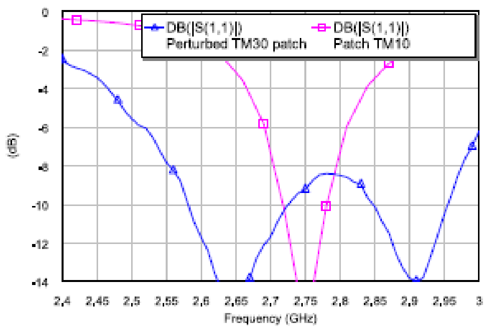

Fig. 6. Measured bandwidth of the patch operating at the perturbed TM30 mode, and a patch operating at the TM10 mode. Both patches are on the same foam-based substrate with a height of 1.3 mm

.

This is a post-print (final draft post-refeering)
Published in final edited form as

Jaume Anguera, Aurora Andújar, Jeevani Jayasinghe. ***High-Directivity Microstrip Patch Antennas Based on TMood-0 Modes****: Antennas and Wireless Propagation Letters, IEEE 2020. Vol.19, Nº1, p. 39-43* https://doi.org/10.1109/LAWP.2019.2952260

element of the array. Therefore, it is interesting to compare the measured bandwidth of these two cases (see Fig. 6). It is shown how the bandwidth at $S11 = -8$ dB is 15.2% and 3.6% for the perturbed TM30 patch and TM10 patch, respectively. This represents four times more bandwidth, which is an advantage of the proposed technique.

Radiation patterns and directivities are measured inside an anechoic chamber (Satimo Stargate-32). The directivity is measured using a three-dimensional pattern integration confirming the simulation results. The measured directivity of 14.6 dB is obtained in comparison with the 15 dB predicted by the simulation (see Fig. 7). There is still room for further improvement to investigate how the secondary lobes can be reduced in order to increase directivity.

V. Discussion

Several techniques to achieve a high directivity using a singlelayer microstrip antenna are compared (see Fig. 8). As expected, the larger the area of the patch, the larger the directivity. The área of the patch antenna at the central frequency of an operation is considered without including the ground plane.

When directivities larger than 15 dB are considered, it is observed that the technique presented in [8] provides the highest directivity. For an area of $4\lambda 0$ 2, it gives a directivity of 18.6 dB, which is larger than the design presented in this letter, which gives a directivity of 18 dB for an area of $5.2\lambda 0$ 2. However, the $S11 < -10$ dB bandwidth for the patch in [8] is only 0.36% showing a narrowband performance. In contrast, for the design presented in this letter, the bandwidth is 4.9%, with very similar electrical height ($0.028\lambda 0$ for [8], and $0.015\lambda 0$ in the proposed design here). Therefore, the presented technique is useful to design the microstrip antennas with large directivities and a sufficient bandwidth to satisfy practical applications.

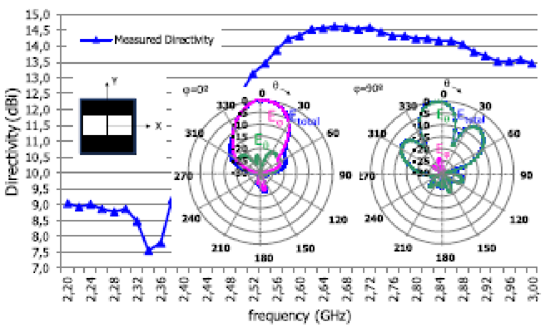

Fig. 7. Measured directivity and radiation patterns at $\phi = 0°$ and $\phi = 90°$.

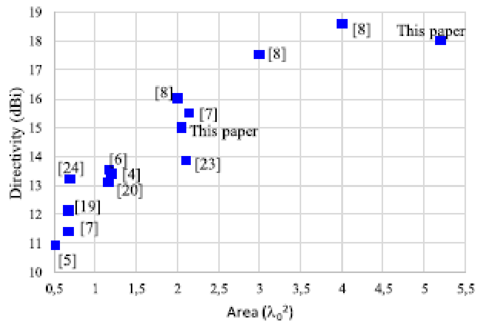

Fig. 8. Directivities of the single-layer patch antennas using different techniques.

VI. Conclusion

A technique to obtain the high-directive broadside radiation patterns for the microstrip patch antennas has been presented. It proposes removing the conductive portions of the radiating patch of the microstrip antennas operating at higher order TModd-0 modes to eliminate the out-of-phase current.

Two microstrip patch antennas operating at TM30 and TM50 modes have been presented showing directivities of 15 and 18 dB, respectively. A prototype has been built for the design operating at the TM30 mode where a measured directivity of 14.6 dB is obtained. The measured bandwidth is four times the bandwidth of an equivalent array of square patches occupying the same area operating in its fundamental mode.

This is a post-print (final draft post-refeering)
Published in final edited form as

Jaume Anguera, Aurora Andújar, Jeevani Jayasinghe. ***High-Directivity Microstrip Patch Antennas Based on TMood-0 Modes****: Antennas and Wireless Propagation Letters, IEEE 2020. Vol.19, Nº1, p. 39-43* https://doi.org/10.1109/LAWP.2019.2952260

The technique can be generalized to the higher order modes following the procedure shown in this letter.

References

[1] D. M. Pozar and D. H. Schaubert, *Microstrip Antennas: The Analysis and Design of Microstrip Antennas and Arrays*. New York, NY, USA: Wiley, 1995.
[2] D. C. Nascimento and J. C. da Lacava, "Design of arrays of linearly polarized patch antennas on an FR4 substrate," *IEEE Antennas Propag. Mag.*, vol. 57, no. 4, pp. 12–22, Aug. 2015.
[3] C. Borja, G. Font, S. Blanch, and J. Romeu, "High directivity fractal boundary microstrip patch antenna," *Electron. Lett.*, vol. 36, no. 9, pp. 778–779, Apr. 2000.
[4] C. Borja and J. Romeu, "On the behavior of Koch island fractal boundary microstrip patch antenna," *IEEE Trans. Antennas Propag.*, vol. 51, no. 6, pp. 1281–1291, Jun. 2003.
[5] J. Anguera, C. Puente, C. Borja, R. Montero, and J. Soler, "Small and high directivity bowtie patch antenna based on the sierpinski fractal," *Microw. Opt. Technol. Lett.*, vol. 31, no. 3, pp. 239–241, 2001.
[6] J. Anguera *et al.*, "Metallized foams for fractal-shaped microstrip antennas," *IEEE Antennas Propag. Mag.*, vol. 50, no. 6, pp. 20–38, Dec. 2008.
[7] J.Anguera,A.Andújar, S. Benavente, J. Jayasinghe, and S. Kahng, "Highdirectivity microstrip antenna with Mandelbrot fractal boundary," *Microw., Antennas Propag.*, vol. 12, no. 4, pp. 569–575, Mar. 2018.
[8] E. El-Khouly, H. Ghali, and S. A. Khamis, "High directivity antenna using a modified peano space-filling curve," *IEEE Antennas Wireless Propag. Lett.*, vol. 6, pp. 405–407, 2007.
[9] A. Pirhadi, F.Keshmiri, M. Hakkak, andM.Tayarani, "Analysis and design of dual band high directivityEBGresonator antenna using square loop FSS as superstrate layer," *Prog. Electromagn. Res.*, vol. PIER 70, pp. 1–20, 2007.
[10] A. Pirhadi, H. Bahrami, and J. Nasri, "Wideband high directive aperture coupled microstrip antenna design by using a FSS superstrate layer," *IEEE Trans. Antennas Propag.*, vol. 60, no. 4, pp. 2101–2106, Apr. 2012.
[11] H. Zhou *et al.*, "A novel high-directivity microstrip patch antenna based on zero-index metamaterial," *IEEE Antennas Wireless Propag. Lett.*, vol. 8, pp. 538–541, 2009.
[12] H. D. Yang, N. G. Alexopoulos, and E. Yablonovitch, "Photonic band-gap materials for high-gain printed circuit antennas," *IEEE Trans. Antennas Propag.*, vol. 45, no. 1, pp. 185–187, Jan. 1997.
[13] R. Weily, T. S. Bird, and Y. J. Guo, "A reconfigurable high-gain partially reflecting surface antenna," *IEEE Trans. Antennas Propag.*, vol. 56, no. 11, pp. 3382–3390, Nov. 2008.
[14] F. Qin, S. Gao, G.Wei, Q. Luo, and C. Gu, "Wideband high directivity circularly polarized Fabry-Perot antenna," in *Proc. Loughborough Antennas Propag. Conf.*, Loughborough, U.K., 2014, pp. 254–258.
[15] A. Pirhadi, M. Hakkak, F. Keshmiri, and R. Karimzadeh Baee, "Design of compact dual band high directive electromagnetic bandgap (EBG) resonator antenna using artificial magnetic conductor," *IEEE Trans. Antennas Propag.*, vol. 55, no. 6, pp. 1682–1690, Jun. 2007.
[16] N. Guérin, S. Enoch, G. Tayeb, P. Sabouroux, P. Vicent, and H. Legay, "A metallic Fabry–Perot directive antenna," *IEEE Trans. Antennas Propag.*, vol. 54, no. 1, pp. 220–224, Jan. 2006.
[17] Y. Liu, H. Gu, and X. Zhao, "Enhanced transmission and high-directivity radiation based on composite right/left-handed transmission line structure," *IEEE Antennas Wireless Propag. Lett.*, vol. 10, pp. 658–661, 2011.
[18] M. U. Azfal and K. P. Esselle, "A low-profile printed planar phase correcting surface to improve directive radiation characteristics of electromagnetic band gap resonator antennas," *IEEE Trans. Antennas Propag.*, vol. 64, no. 1, pp. 276–280, Jan. 2016.
[19] J. M. J. W. Jayasinghe, J. Anguera, and D.N. Uduwawala, "Genetic algorithm optimization of a high-directivity microstrip patch antenna having a rectangular profile," *Radioengineering*, vol. 22, no. 3, pp. 700–707, Sep. 2013.
[20] J. M. J. W. Jayasinghe, J. Anguera, D. N. Uduwawala, and A. Andújar, "Highdirectivity genetic microstrip patch antenna," *Int. J. Electron. Lett.*, 2015, doi: 10.1080/21681724.2015.1034189.
[21] X. Zhang and L. Zhu, "Gain-enhanced patch antennas with loading of shorting pins," *IEEE Trans. Antennas Propag.*, vol. 64, no. 8, pp. 3310– 3318, Aug. 2016.
[22] X. Zhang and L. Zhu, "Gain-enhanced patch antenna without enlarged size via loading of slot and shorting pins," *IEEE Trans. Antennas Propag.*, vol. 65, no. 11, pp. 5701–5709, Nov. 2017.
[23] P. Juyal and L. Shafai, "Sidelobe reduction of TM12mode of circular patch via non resonant narrow slot," *IEEE Trans. Antennas Propag.*, vol. 64, no. 8, pp. 3361–3369, Aug. 2016.
[24] X. Zhang, L. Zhu, and Q. S. Wu, "Sidelobe-reduced and gain-enhanced square patch antennas with adjustable beamwidth under TM03 mode operation," *IEEE Trans. Antennas Propag.*, vol. 66, no. 4, pp. 1704–1713, Apr. 2018.
[25] C. Balanis, *Antenna Theory and Design*, 2nd ed. New York, NY, USA: Wiley, 1997.